Highpower cw verticalcavity top surfaceemitting GaAs quantum well lasers

B. Tell, Y. H. Lee, K. F. BrownGoebeler, J. L. Jewell, R. E. Leibenguth et al.

Citation: Appl. Phys. Lett. **57**, 1855 (1990); doi: 10.1063/1.104038
View online: http://dx.doi.org/10.1063/1.104038
View Table of Contents: http://apl.aip.org/resource/1/APPLAB/v57/i18
Published by the American Institute of Physics.

Additional information on Appl. Phys. Lett.

Journal Homepage: http://apl.aip.org/
Journal Information: http://apl.aip.org/about/about_the_journal
Top downloads: http://apl.aip.org/features/most_downloaded
Information for Authors: http://apl.aip.org/authors

ADVERTISEMENT

Downloaded 16 Apr 2013 to 143.248.118.122. This article is copyrighted as indicated in the abstract. Reuse of AIP content is subject to the terms at: http://apl.aip.org/about/rights_and_permissions

High-power cw vertical-cavity top surface-emitting GaAs quantum well lasers

B. Tell, Y. H. Lee, K. F. Brown-Goebeler, and J. L. Jewell
AT&T Bell Laboratories, Holmdel, New Jersey 07733

R. E. Leibenguth, M. T. Asom, G. Livescu, L. Luther, and V. D. Mattera
AT&T Bell Laboratories, STC, Breinigsville, Pennsylvania 18031

(Received 16 July 1990; accepted for publication 23 August 1990)

We have devised a novel vertical-cavity top surface-emitting GaAs quantum well laser structure which operates at 0.84 μm. The laser combines peripheral current injection with efficient heat removal and uses only the epitaxially grown semiconductor layers for the output mirrors. The structure is obtained by a patterned deep H^+ implantation and anneal cycle which maintains surface conductivity while burying a high resistance layer. Peripheral injection of current occurs from the metallized contact area into the nonimplanted nonmetallized emission window. For 10-μm-diam emitting windows, $\sim$4 mA thresholds with continuous-wave (cw) room-temperature output powers >1.5 mW are obtained. Larger diameter emitting windows have maximum cw output powers greater than 3 mW. These are the highest cw powers achieved to date in current injected vertical-cavity surface-emitting lasers.

Vertical-cavity surface-emitting lasers (VCSELs) are of great potential interest for a wide variety of device applications, including communications, optical switching and computing, optical interconnects, image processing, etc. Recently, continuous operation at room temperature has been achieved by several groups,[1-6] but the simultaneous realization of low-threshold currents (~ 1 kA/cm^2) and moderate output power (>1 mW) has not been previously achieved. Although high reflectivity mirrors of the distributed Bragg reflector (DBR) type can be grown entirely of quarter-wave layers of high and low index semiconductors,[7] the usual structure has also employed hybrid dielectric mirrors and or metallic mirrors.[1-5] This is mainly due to the high resistance of the p-type DBR of thickness necessary to produce the desired reflectivity ($>99\%$). Elimination of the p mirror or reduction of its thickness requires a hybrid dielectric (e.g., and SiO_2-TiO_2) and metal,[1-3] or metal alone.[4,5] If the top metal is semitransparent, top surface emission can be obtained.[5] Otherwise, the laser output must be obtained through the substrate. In the GaAs system, this requires etching holes in the substrate[1,3] or the use of strained layers of $In_yGa_{1-y}As$ with $y \simeq 0.2$ to red shift the wavelength in order to render the substrate semitransparent.[2,4]

We have developed a novel self-aligned single mask level scheme to produce efficient peripheral current injection into and heat removal from an emitting window region of a VCSEL.[6] A buried damage implant encloses the emitting area and results in a funneling type carrier injection from the peripheral region as illustrated in Fig. 1(a). A top view of a laser with a 10-μm-diam window is shown in Fig. 1(b). The necessary reflectivity in the window region is achieved entirely by molecular beam epitaxially (MBE) grown mirrors, and does not require either thin metallization or hybrid dielectrics. Improved control of the MBE growth and of the processing procedures has enabled achievements of continuous-wave (cw) room-temperature thresholds of 3.5–4 mA with 10-μm-diam structures with power up to 1.5 mW. Larger diameter structures have lower threshold current densities and cw power above 3 mW. All lasing characteristics and spectra discussed in this letter are cw at room temperature.

The MBE-grown structure contains the p-doped DBR top mirror, the n-doped DBR bottom mirror, and GaAs

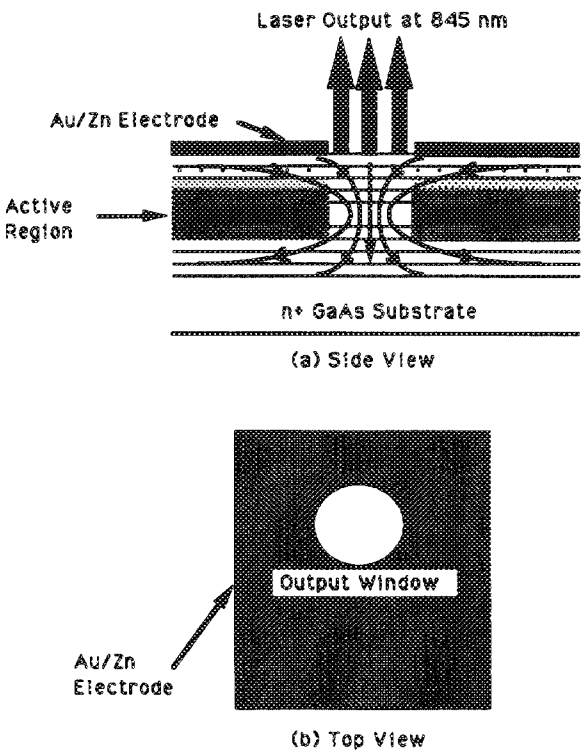

FIG. 1. (a) Schematic view of the current flow (thin arrows) and the laser output, where the shading tone indicates the vertical ion damage profile. (b) A schematic top view of the structure showing the window with the surrounding contact area which in the present work was 40 μm$\times$60 μm. Individual lasers were isolated by etching grooves to the depth of the active layer.

 0003-6951/90/441855-03$02.00 © 1990 American Institute of Physics

Downloaded 16 Apr 2013 to 143.248.118.122. This article is copyrighted as indicated in the abstract. Reuse of AIP content is subject to the terms at: http://apl.aip.org/about/rights_and_permissions

four quantum well active region grown on an n^+ [100] GaAs substrate. A transition region of linear grading of the Al concentration joins the active region to the mirror region. The Be-doped top mirror contains 20 pairs of an $Al_{0.16}Ga_{0.84}As/AlAs$ quarter wavelength stack with the thickness adjusted to accommodate thin (10 nm) intermediate gap $Al_{0.58}Ga_{0.42}As$ layers. The top several pairs were doped at 2×10^{19} cm^{-3} to facilitate peripheral injection and contacting, and the intermediate gap layers were introduced to lower the valence-band potential barriers and consequently reduce the series resistance.[4,8] The bottom mirror is a Si-doped (3×10^{18} cm^{-3}) 27-pair $Al_{0.16}Ga_{0.84}As$ quarter wavelength stack. The undoped active region contains four 10 nm GaAs quantum wells and three 7 nm $Al_{0.3}Ga_{0.7}As$ barriers. The total thickness of the active layer, including the grading region, is a full wavelength in the medium.

The structure depicted in Fig. 1(a) was obtained by a patterned implant of H^+ to produce a vertical resistance profile with a maximum resistance slightly above the active layer. In order to selectively implant H^+ to a depth of 2.5 μm in AlGaAs, a blocking structure of $\sim$6 μm of resist is required.[9] A multilevel resist mask consisting of 0.3 μm SiO_2, 6 μm of hard baked photoresist ($\sim$200 °C for 1 h), 0.1 μm thermally evaporated Cr, and thin standard positive photoresist was employed. Circular windows of 10, 15, 20, and 30 μm diameter were protected by the thin resist and the pattern transferred to the Cr by wet etching. The thick resist was reactively ion etched in oxygen with the Cr protecting the active window area. Following removal of the SiO_2 in the contact region with HF, Au-Zn was thermally evaporated across the entire wafer. Hydrogen ions were implanted at 300 keV to a dose of 2.5×10^{14} cm^{-2} through the Au-Zn contact, and blocked in the window area by the combination of metal, hard-baked resist, and SiO_2. Following implantation, the sample was placed in hot-resist stripper, which lifted off the photoresist and metal from the window region, resulting in the pattern shown in Fig. 1(b). After plating a Au-Sn contact to the n^+ substrate, the structure was annealed at $\sim$475 °C for 30 s. TRIM calculations[9] show the region of maximum damage (given by a displacement density) occurs at a depth of $\sim$2.5 μm, with the displacement density reduced by more than one order of magnitude in the near-surface region. Prior to the anneal, the structure is highly resistive (passing only $\sim\mu$A at several volts forward bias). The anneal serves both to alloy the contacts and to further shape the resistance profile by further reducing the surface resistance while retaining a high resistance layer under the metallized region. Prior to testing, the lasers are In soldered with substrate down to a Cu plate.

The *L-I* and *V-I* curves for a 10-μm-diam emitting window laser are shown in Fig. 2. The threshold current and voltage for this laser are 4.2 mA and 3.8 V, respectively. The saturation cw power for this laser is $>$1.5 mW, with 1 mW output power obtained at 1 mA above threshold. Near threshold, the laser emits in the lowest order Gaussian mode (TEM_{00})[10] but shifts to a higher order mode above 0.5 mW as evidenced by the kink in the *L-I* curve. The slope of the *L-I* curve for emission in the lowest order mode is 0.5 mW/0.4 mA. While the slope of the *L-I* curve (especially for the 10-μm-diam emitter windows) can be greater than 1 mW/mA, the differential quantum efficiency is not as high as this slope would indicate (i.e., $>$0.7). It appears that the transmission peak at the Fabry–Perot resonance is at the low-energy side of the peak of the gain curve. With the temperature rise during cw operation, the peak of the gain curve (with a larger red shift per unit temperature increase than the Fabry–Perot mode) passes through the Fabry–Perot mode, resulting in a large initial increase in light intensity near threshold and a subsequent decrease in intensity at higher currents.[6] This explanation results from the observation that under short pulse low duty cycle conditions, the slope of the pulsed *L-I* curve (for output less than 1 mW) is less than for the cw case, and the slope increases with an increase in pulse width. The interpretation of these *L-I* curves and the resulting differential quantum efficiency is still under study.

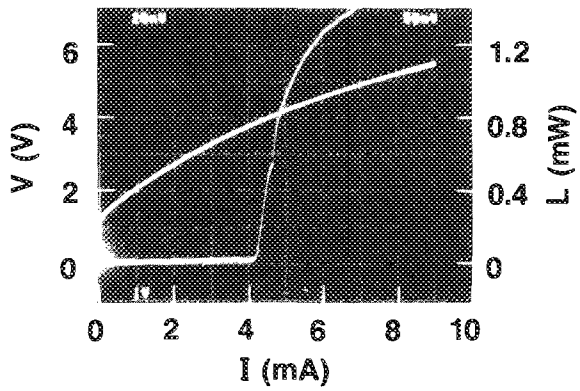

FIG. 2. *L-I* and *V-I* curves for a 10-μm-diam laser exhibiting high *L-I* slope efficiency.

The *L-I* curve for a different laser with a 10-μm-diam window is shown in the inset of Fig. 3. A sharp lasing threshold occurs around 3.6 mA. The spectra obtained just below (3.5 mA) and just above threshold (3.7 mA) are

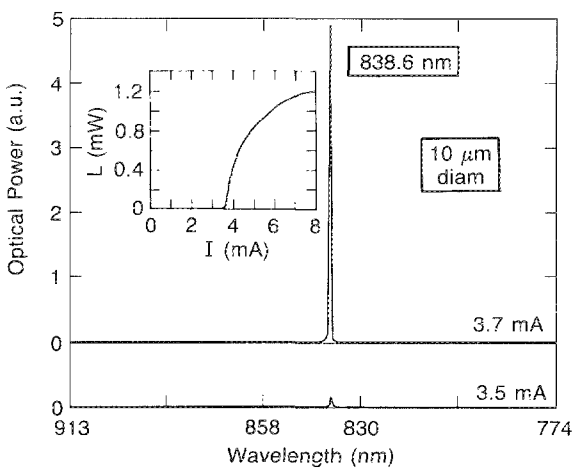

FIG. 3. Emission spectra at $\sim$ 0.1 mA below and above threshold for a 10-μm-diam laser for which the *L-I* curve is shown in the inset.

Downloaded 16 Apr 2013 to 143.248.118.122. This article is copyrighted as indicated in the abstract. Reuse of AIP content is subject to the terms at: http://apl.aip.org/about/rights_and_permissions

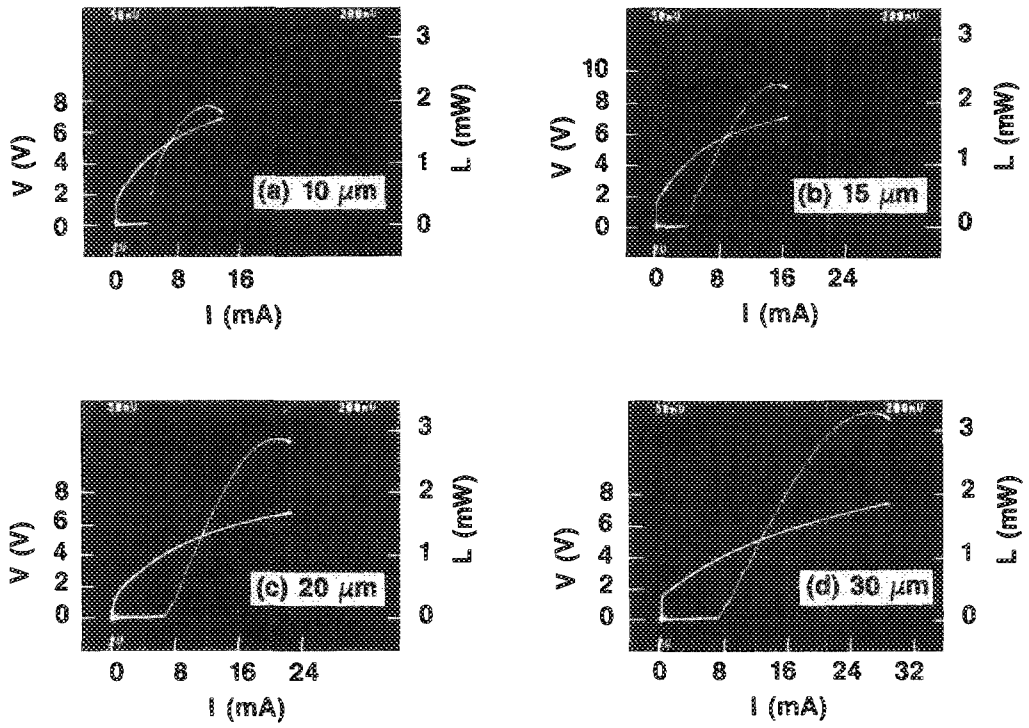

FIG. 4. cw room-temperature *V-I* and *L-I* curves for adjacent lasers with the four different diameter emitting windows.

also shown in Fig. 3 on the same linear intensity scale, but shifted vertically for clarity. An increase of $\geqslant 50$ in light intensity is observed as current is increased from 0.1 mA below threshold to 0.1 mA above threshold. The laser linewidth has been measured with a scanning Fabry–Perot étalon and is less than 0.02 nm. Only one Fabry–Perot mode is observed due to the short cavity length.

Higher cw powers and lower threshold current densities are obtained with larger emitting areas. In Figs. 4(a)–4(d) are shown the *V-I* and *L-I* curves for adjacent lasers with the four different diameter emitting windows. The threshold currents increase from 4 to 7.5 mA as the area increases, corresponding to threshold current densities of 5.1–1.1 kA/cm^2. Both the 10 and 15 μm emitting window structures show large slopes of the *L-I* curves near the threshold, with a decreasing slope at higher currents. The larger emitting windows exhibit a more constant slope over a larger *L-I* range.For output power up to 2 mW, the slope of the *L-I* curve gives differential quantum efficiencies of 0.2 and 0.16 for for the 20 and 30 μm structures, respectively. The increased threshold current density for the smaller diameter appears to arise from a combination of diffraction loss due to poorer optical guiding and nonradiative recombination at the periphery which are more severe for smaller diameter structures. On the other hand, the maximum emitted power per unit area is larger for the smaller structures, indicating superior heat removal. The smaller structures have a larger circumference to area ratio, so that heat removal is more efficient.

In conclusion, we have demonstrated the first vertical-cavity surface-emitting lasers with room-temperature cw powers above 1 mW and with threshold current densities in the low kA/cm^2 range. We believe further improvements in processing and material growth will further improve these characteristics and allow high-power addressable arrays, etc.

[1] F. Koyama, S. Kinoshita, and K. Iga, Appl. Phys. Lett. **55**, 221 (1989).
[2] Y. H. Lee, J. L. Jewell, A. A. Scherer, S. L. McCall, J. P. Harbison, and L. T. Florez, Electron. Lett. **25**, 1377 (1989).
[3] K. Tai, R. J. Fischer, C. W. Seabury, N. A. Olsson, T. D. C. Hus, Y. Ota, and A. Y. Cho, Appl. Phys. Lett. **55**, 2473 (1989).
[4] R. S. Geels, S. W. Corzine, J. W. Scott, D. B. Young, and L. A. Coldren, IEEE Photon. Tech. Lett. **2**, 234 (1990).
[5] E. F. Schubert, L. W. Tu, R. F. Kopf, G. J. Zydzik, and D. G. Deppe, Appl. Phys. Lett. **57**, 117 (1990).
[6] Y. H. Lee, B. Tell, K. F. Brown-Goebeler, J. L. Jewell, and J. V. Hove, Electron. Lett. **26**, 710 (1990).
[7] J. P. Vander Ziel and M. Ilegems, Appl. Opt. **15**, 1256 (1976).
[8] K. Tai, L. Yang, Y. H. Wang, J. D. Wynn, and A. Y. Cho, Appl. Phys. Lett. **56**, 2496 (1990).
[9] J. F. Ziegler, J. P. Biersack, and U. Littmark, *The Stopping and Range of Ions in Solids* (Pergamon, New York, 1984), Vol. 1. Various computer programs based on this model are available. We used a version called TRIM 88.
[10] C. J. Chang-Hasnain, M. Orenstein, A. Von Lehmen, L. T. Florez, J. P. Harbison, and N. G. Stoffel, Appl. Phys. Lett. **57**, 218 (1990).

Downloaded 16 Apr 2013 to 143.248.118.122. This article is copyrighted as indicated in the abstract. Reuse of AIP content is subject to the terms at: http://apl.aip.org/about/rights_and_permissions